Available online at www.sciencedirect.com
ScienceDirect
Journal of Hazardous Materials 143 (2007) 95–101
Journal of Hazardous Materials
www.elsevier.com/locate/jhazmat

Removal of C.I. Acid Orange 7 from aqueous solution by UV irradiation in the presence of ZnO nanopowder

N. Daneshvar *, M.H. Rasoulifard [1], A.R. Khataee [1], F. Hosseinzadeh [1]

Water and Wastewater Treatment Research Laboratory, Department of Applied Chemistry, Faculty of Chemistry, University of Tabriz, Tabriz, Iran

Received 12 July 2006; received in revised form 29 August 2006; accepted 30 August 2006
Available online 3 September 2006

Abstract

The removal of C.I. Acid Orange 7 (AO7) from aqueous solution under UV irradiation in the presence of ZnO nanopowder has been studied. The average crystallite size of ZnO powder was determined from XRD pattern using the Scherrer equation in the range of 33 nm. The experiments showed that ZnO nanopowder and UV light had a negligible effect when they were used on their own. The effects of some operational parameters such as pH, the amount of ZnO nanopowder and initial dye concentration were also examined. The photodegradation of AO7 was enhanced by the addition of proper amount of hydrogen peroxide, but it was inhibited by ethanol. From the inhibitive effect of ethanol, it was deducted that hydroxyl radicals played a significant role in the photodegradation of the dye. The kinetic of the removal of AO7 can be explained in terms of the Langmuir–Hinshelwood model. The values of the adsorption equilibrium constant, K_{AO7}, and the kinetic rate constant of surface reaction, k_c, were 0.354 $(mg\,l^{-1})^{-1}$ and 1.99 $mg\,l^{-1}\,min^{-1}$, respectively. The electrical energy consumption per order of magnitude for photocatalytic degradation of AO7 was lower in the UV/ZnO/H_2O_2 process than that in the UV/ZnO process. Accordingly, it could be stated that the complete removal of color, after selecting desired operational parameters could be achieved in a relatively short time, about 60 min.

Keywords: Advanced oxidation processes; Kinetic model; Zinc oxide nanopowder; C.I. Acid Orange 7; Electricity consumption

1. Introduction

Wastewater from textile, paper and some other industries contain residual dyes, which are not readily biodegradable. Adsorption and chemical coagulation processes are two common techniques of wastewater treatment. However, these methods merely transfer dyes from the liquid to the solid phase causing secondary pollution and requiring further treatment. Advanced oxidation processes (AOPs) are alternative techniques of destruction of dyes and many other organics in wastewater and effluents. These processes generally, involve UV/H_2O_2, UV/O_3 or UV/Fenton's reagent for the oxidative degradation of contaminants. Semiconductor photocatalysis is another developed AOP, which can be conveniently applied to remove of different organic pollutants [1–4].

TiO_2 and ZnO nanopowder especially in recent years, are used as effective, inexpensive and nontoxic semiconductor photocatalysts for the degradation of a wide range of organic chemicals and synthetic dyes. The size of photocatalysts is one of the most important factors. There were many comparative studies about the photocatalytic efficiency of pollutants between TiO_2 and ZnO, which emphasized the effectiveness of TiO_2 or ZnO. In these studies, Degauss (P-25) TiO_2 (mean diameter, 25 nm) and commercial ZnO (mean diameter, 200 nm) are the most commonly used effective photocatalysts. However, the problem is the great size discrepancy of the two different kinds of photocatalysts [5–10].

ZnO nanopowder appears to be a suitable alternative to TiO_2 since its photodegradation mechanism has been proven to be similar to that of TiO_2 [4]. ZnO nanopowder has been reported, sometimes, to be more efficient than TiO_2. Its efficiency has been reported to be particularly noticeable in the advanced oxidation of pulp mill bleaching wastewater [11,12], the photooxidation of 2-phenylphenol and photocatalysed oxidation of phenol [3]. The biggest advantage of ZnO in comparison with TiO_2 is it adsorbs over a larger fraction of UV

* Corresponding author. Tel.: +98 411 3393146; fax: +98 411 3393038.
E-mail addresses: nezam_daneshvar@yahoo.com (N. Daneshvar), m_h_rasoulifard@yahoo.com (M.H. Rasoulifard), ar_khataee@yahoo.com (A.R. Khataee).
[1] Tel.: +98 411 3393165; fax: +98 411 3393038.

0304-3894/$ – see front matter © 2006 Elsevier B.V. All rights reserved.
doi:10.1016/j.jhazmat.2006.08.072

spectrum and the corresponding threshold of ZnO is 425 nm [13].

The aim of the present work is to study the removal of an azo dye, C.I. Acid Orange 7, extensively used by the textile industry, in the presence of ZnO nanopowder as a suitable alternative to TiO_2 irradiated by UV-C light (UV/ZnO process). The effect of UV light irradiation, pH and the amount of nanocatalyst was examined. The effect of the addition of H_2O_2 was also studied for enhancing the elimination of the azo dye. The inhibitive influence of ethanol, commonly used to quench hydroxyl radicals, provides information on reactive species involved in the reaction. The EE/0 "Electrical Energy per Order" was calculated and showed that a moderated efficiency was obtained in UV/ZnO Process. A detailed kinetic description of the process was given based on well-known mechanistic/kinetic models namely: the Langmuir–Hinshelwood (L–H) model whereby the organic regent was pre-adsorbed on photocatalyst surface prior to UV illumination.

2. Experiments and methods

2.1. Materials

The average crystallite size (D in nm) of ZnO nanopowder was determined from XRD pattern of the ZnO nanopowder (Fig. 1) according to the Scherrer equation: $D = k(\lambda/\beta \cos\theta)$ where k is a constant equal to 0.89, λ the X-ray wavelength equal to 0.154 nm, β the full width at half maximum and θ the half diffraction angle (17.61) [14]. The average particle size is about 33 nm by calculation, surface area is 5 $m^2\,g^{-1}$ and band gap energy is 3.2 eV. ZnO nanoparticles obtained from Merck Co. (Germany). C.I. Acid Orange 7 (AO7) was purchased from Boyakhsaz Co. (Iran). The structure of AO7 has been depicted in Fig. 2. Sulfuric acid, sodium hydroxide and hydrogen peroxide were obtained from Merck Co. (Germany). Ethanol (99%) was purchased from Aldrich Co. (England).

2.2. Procedures

For the photodegradation of AO7, a solution containing known concentration of the dye and ZnO nanopowder was prepared and it was allowed to equilibrate for 30 min in the darkness, then 50 ml of the prepared suspension was transferred to a 500 ml Pyrex reactor. Irradiation was carried out with a 30 W (UV-C, 254 nm) mercury lamp (Philips), which was put above the batch photoreactor. The distance between solution and UV source was constant, 15 cm, in all experiments. The light intensity in the center of the photoreactor was measured by a Lux-meter, Leybold-Heraeus (0.55 kLux). The suspension pH values were adjusted at desired level using dilute NaOH and H_2SO_4 and then the pH values were measured with pH meter (Philips PW 9422). After that, the lamp was switched on to initiate the reaction. During irradiation, agitation was maintained by a magnetic stirrer (Ogawa Seiki) to keep the suspension homogeneous, and the suspension was sampled after an appropriate illumination time. The concentration of the dye in each degraded sample was determined with a spectrophotometer (UV/Vis Spectrophotometer, Perkin-Elmer 550 SE) at $\lambda_{max} = 485$ nm and a calibration curve. By this method conversion percent of AO7 can be obtained in different intervals. Then the degree of photodegradation (X) as a function of time was calculated.

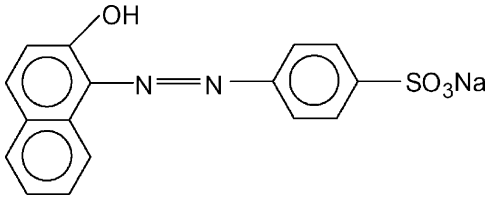

Fig. 2. Structure of C.I. Acid Orange 7 (C.I. No. 15510).

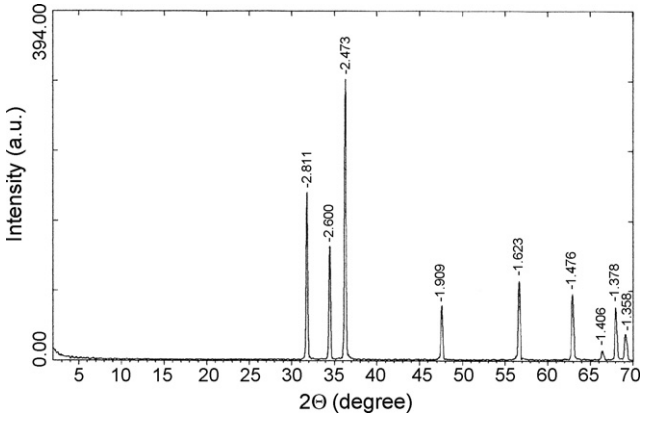

Fig. 1. XRD pattern of ZnO nanoparticles.

3. Results and discussion

3.1. Effect of UV irradiation and ZnO nanoparticles

The change in the dye concentration versus time profile during the photocatalytic degradation of AO7 is shown in Fig. 3. The removal of AO7 was negligible in the absence of ZnO nanopow-

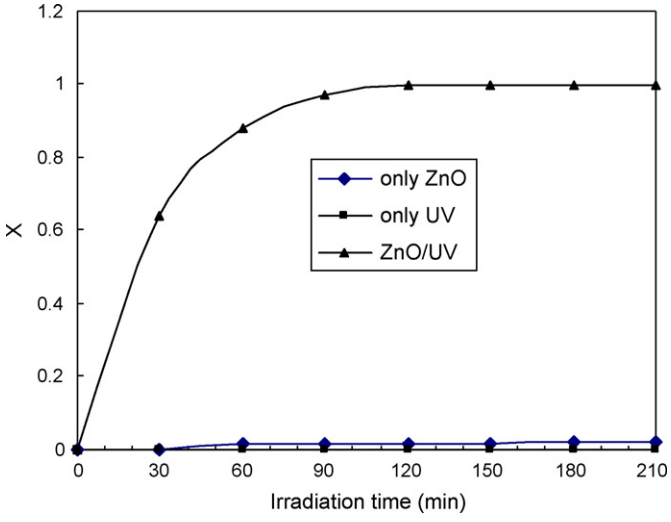

Fig. 3. Effect of UV light and ZnO nanoparticals on photocatalytic degradation of AO7. $[AO7]_0 = 20\,mg\,l^{-1}$; $[ZnO] = 160\,mg\,l^{-1}$; pH neutral.

der. It can be seen from the figure that in the presence of both ZnO nanopowder and light 100% of dye was degraded at the irradiation time of 60 min. These experiments demonstrated that both UV light and a photocatalyst, such as ZnO were needed for the effective destruction of AO7. Because it has been established that the photocatalytic degradation of organic matter in solution is initiated by photoexcitation of the semiconductor, followed by the formation of an electron–hole pair on the surface of catalyst Eq. (1). The high oxidative potential of the hole (h_{VB}^+) in the catalyst permits the direct oxidation of organic matter (dye) to reactive intermediates Eq. (2). Very reactive hydroxyl radicals can also be formed either by the decomposition of water Eq. (3) or by the reaction of the hole with $^-$OH Eq. (4). The hydroxyl radical is an extremely strong, non-selective oxidant that leads degradation of organic chemicals [3,4,13].

$$ZnO + h\nu \rightarrow ZnO\,(e_{CB}^- + h_{VB}^+) \quad (1)$$

$$h_{VB}^+ + \text{dye} \rightarrow \text{oxidation of the dye} \quad (2)$$

$$h_{VB}^+ + H_2O \rightarrow H^+ + {}^\bullet OH \quad (3)$$

$$h_{VB}^+ + OH^- \rightarrow {}^\bullet OH \quad (4)$$

Electron in the conduction band (e_{CB}^-) on the catalyst surface can reduce molecular oxygen to superoxide anion Eq. (5). This radical, in the presence of organic scavengers, may form organic peroxides Eq. (6) or hydrogen peroxide Eq. (7).

$$e_{CB}^- + O_2 \rightarrow {}^\bullet O_2^- \quad (5)$$

$${}^\bullet O_2^- + \text{dye} \rightarrow \text{dye}{-}OO^\bullet \quad (6)$$

$${}^\bullet O_2^- + HO_2^\bullet + H^+ \rightarrow H_2O_2 + O_2 \quad (7)$$

Electrons in the conduction band are also responsible for the production of hydroxyl radicals, which have been indicated as the primary cause of organic matter mineralization Eq. (8) [4,15].

$${}^\bullet OH + \text{dye} \rightarrow \text{degradation of the dye} \quad (8)$$

3.2. Effect of the amount of ZnO nanopowder

The effect of the amount of ZnO nanopowder on the photodegradation efficiency was shown in Fig. 4. Experiments performed with different concentration of ZnO nanopowder showed that the photodegradation efficiency increases with an increase in ZnO nanopowder concentration up to 160 mg l^{-1}, and is then decreased. This observation can be explained in terms of availability of active sites on the catalyst surface and the penetration of UV light into the suspension. The total active surface area increases with increasing catalyst dosage. At the same time, due to an increase in the turbidity of the suspension, there is a decrease in UV light penetration as a result of increased scattering effect and hence the photoactivated volume of suspension decreases [4,13]. Since the most effective decomposition of AO7 was observed with 160 mg l^{-1} of ZnO nanopowder, the other experiments were performed in this concentration of ZnO nanopowder.

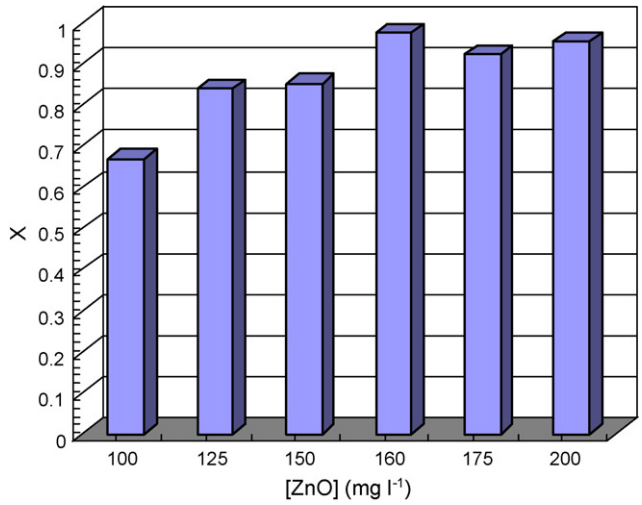

Fig. 4. Effect of ZnO amount on photodegradation efficiency of AO7 at irradiation time of 60 min. $[AO7]_0 = 20$ mg l^{-1}; pH neutral.

3.3. Effect of initial dye concentration

It is important from an application point of view to study the dependence of removal efficiency on the initial concentration of dye. Fig. 5 shows the effect of initial AO7 concentration on photocatalytic degradation efficiency. It can be seen that color removal efficiency decreased as initial dye concentration increased. The presumed reason is that when the initial concentration of dye is increased, more and more dye molecules are adsorbed on the surface of ZnO nanopowder. The large amount of adsorbed dye is thought to have an inhibitive effect on the reaction of dye molecules with photogenerated holes or hydroxyl radicals, because of the lack of any direct contact between them. Once the concentration of dye is increased, it also causes the dye molecules to absorb light and the photons never reach the photocatalyst surface, thus the photocatalytic degradation efficiency decreases [1,16,17].

3.4. Effect of the initial pH

The effect of pH on the photocatalytic degradation efficiency of AO7 was examined in the pH range 2–11 in UV/ZnO pro-

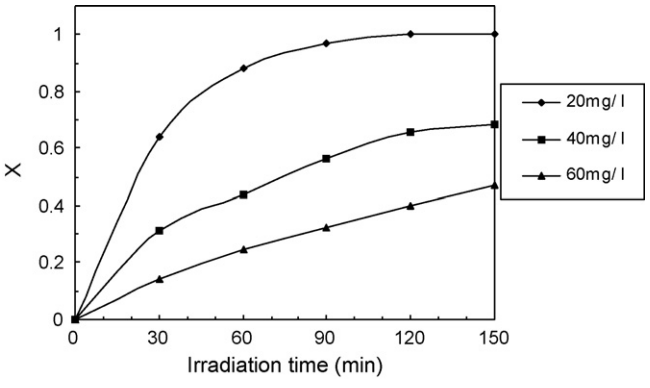

Fig. 5. Effect of initial dye concentration on photocatalytic degradation efficiency of AO7. [ZnO] = 160 mg l^{-1}; pH neutral.

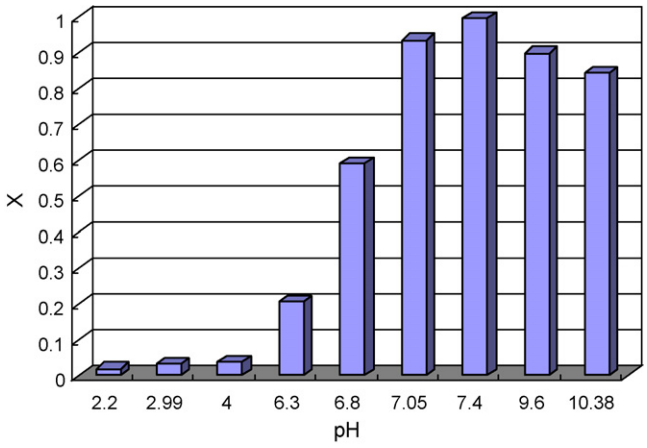

Fig. 6. Effect of pH on photocatalytic degradation of AO7 at irradiation time of 60 min. $[AO7]_0 = 20\,mg\,l^{-1}$; $[ZnO] = 160\,mg\,l^{-1}$.

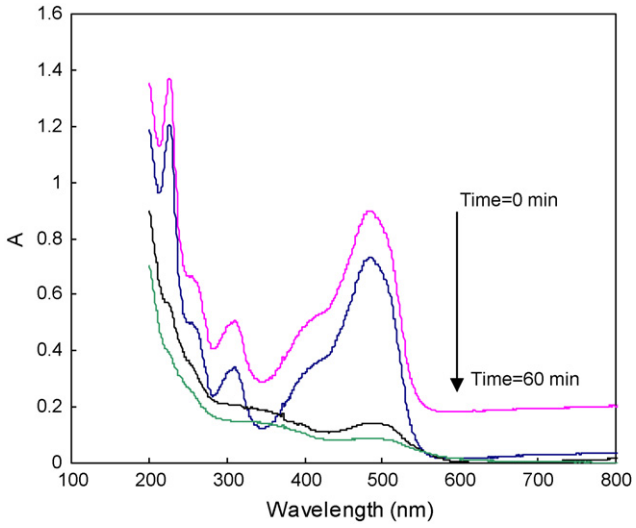

Fig. 7. Spectral changes of AO7 solution during illumination in the presence of ZnO nanoparticles. $[AO7]_0 = 20\,mg\,l^{-1}$; $[ZnO] = 160\,mg\,l^{-1}$; pH neutral.

cess. The results were depicted in Fig. 6. The results showed a direct influence of the pH of the solution on the heterogeneous photocatalysis process. In alkaline solutions photodegradation efficiency was more than that in acidic solutions. It is because photodecomposition of ZnO nanopowder takes place in acidic and neutral solutions. The photocorrosion of ZnO nanopowder is complete at pH lower than 4. At pH higher than 10, no photocorrosion of ZnO nanopowder takes place. More efficient formation of hydroxyl radicals occurs in alkaline solution Eq. (4). On the other hand, AO7 has a sulfuric group in its structure, which is negatively charged in alkaline conditions, therefore, in the alkaline solution dye may not be adsorbed onto photocatalyst surface effectively [1,3,4]. In the light of the findings, it was deduced that the efficient condition for photodegradation of AO7 was neutral pH [4].

3.5. Spectral changes of AO7 during photodestruction

The changes in the absorption spectra of AO7 solutions during the photodestruction process at different irradiation times are shown in Fig. 7. The decrease of the absorption peak of AO7 at 485 nm in Fig. 7 indicated a rapid degradation of azo dye. Complete removal of AO7 was observed after 60 min of irradiation. Also after 20 min the band intensity at 300–310 and 220 nm started to decrease and disappeared after 60 min. The decrease of the absorption peak of AO7 at $\lambda_{max} = 485$ indicated a rapid degradation of the azo dye.

3.6. Kinetics of photocatalytic degradation of AO7

For engineering purposes, it is useful to find out a simple and easy-to-use rate equation that fits the experimental rate data. Since, adsorption is considered critical in the heterogeneous photocatalytic oxidation process, the Langmuir–Hinshelwood model was used to describe the photooxidation kinetics of dyes by a few previous researchers. This treatment is subject to the assumptions that sorption of both the oxidant and the reductant is a rapid equilibrium process and that the rate-determining step of the reaction involves both species present in a monolayer at the solid–liquid interface [1].

Photodegradation experiments of AO7 by UV/ZnO process exhibited pseudo-first-order kinetics with respect to the concentration of the organic compound

$$-\frac{d[AO7]}{dt} = k_{obs}[AO7] \tag{9}$$

whose integration gives, for $[AO7] = [AO7]_0$ at $t = 0$:

$$\ln\left(\frac{[AO7]_0}{[AO7]}\right) = k_{obs}t \tag{10}$$

in which k_{obs} is the pseudo-first-order rate constant.

Fig. 8 shows a plot of $\ln([AO7]_0/[AO7])$ versus time for all the experiments with different initial concentration of AO7. By applying a least square regression analysis the values of k_{obs} have been obtained. Table 1 reports the values of k_{obs} for all experiments carried out. The reaction rate proceeds according to pseudo-first-order kinetics with a kinetic constant, which decreases as the initial reactant concentration. This can be ascribed to the decrease in the number of active sites on the catalyst surface due to the covering of the surface with AO7

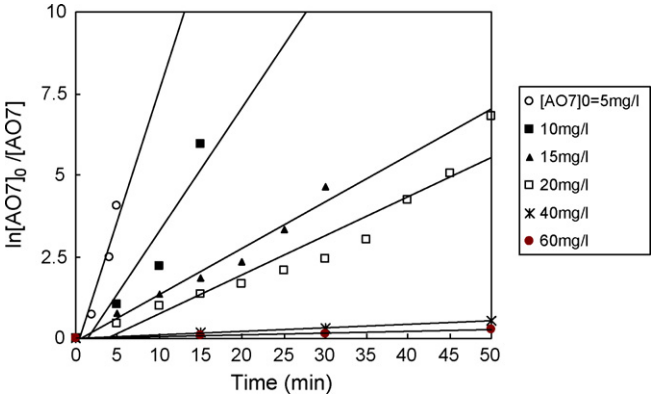

Fig. 8. Determination of the pseudo-first-order kinetic rate constants, k_{obs}.

Table 1
AO7 conversion (at 5 min) and pseudo-first-order kinetic rate constants in photocatalytic experiments with different initial concentration

Experiment number	$[ZnO]_0$ (mg l^{-1})	$[AO7]_0$ (mg l^{-1})	X_5 (%)	k_{obs} (min^{-1})	$1/k_{obs}$ (min)	r^2
1	160	60	2.6	0.034	28.6	0.96
2	160	40	5.5	0.056	17.7	0.98
3	160	20	37	0.120	8.326	0.92
4	160	15	45.6	0.143	7.002	0.97
5	160	10	63.9	0.381	2.625	0.89
6	160	5	95	0.697	1.434	0.93

molecules, which is directly proportional with the initial concentration of AO7. The relationship between the initial degradation rate (r) and the initial concentration of organic substrate for heterogenous photocatalytic degradation process has been described by Langmuir–Hinshelwood model, which can be written as follows:

$$r = k_c \frac{K_{AO7}[AO7]}{1 + K_{AO7}[AO7]_0} = k_{obs}[AO7] \quad (11)$$

$$\frac{1}{k_{obs}} = \frac{1}{k_c K_{AO7}} + \frac{[AO7]_0}{k_c} \quad (12)$$

where K_{AO7} is the Langmuir–Hinshelwood adsorption equilibrium constant.

The data reported in Table 1 were plotted in Fig. 9 as $1/k_{obs}$ versus $[AO7]_0$. By means of a least square best fitting procedure, the values of the adsorption equilibrium constant, K_{AO7}, and the kinetic rate constant of surface reaction, k_c, were calculated [3,11]. The values were $K_{AO7} = 0.354\,(\text{mg l}^{-1})^{-1}$ and $k_c = 1.99\,\text{mg l}^{-1}\,\text{min}^{-1}$. Behnajady and his co-workers reported Langmuir–Hinshelwood equation constants for decolorization of the solution containing C.I. Acid Yellow 23 (40 mg l^{-1}) in the presence of ZnO (750 mg l^{-1}). The values are $K_{dye} = 3.15\,(\text{mg l}^{-1})^{-1}$ and $k_c = 0.913\,\text{mg l}^{-1}\,\text{min}^{-1}$ [13]. Dutta and Chakrabarti proposed a rate equation based on Langmuir–Hinshelwood model for photocatalytic degradation of two textile dyes in wastewater using ZnO as semiconductor catalyst. The values of Langmuir–Hinshelwood equation constants of Methylene Blue and Eosin Y are 0.0345 and $0.0859\,(\text{mg l}^{-1})^{-1}$, respectively [18].

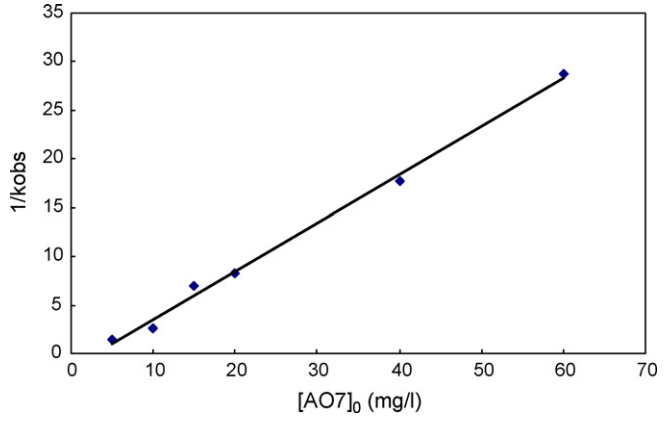

Fig. 9. Determination of the adsorption equilibrium constant, K_{AO7} and the second order rate constant, k_c for the Langmuir–Hinshelwood kinetic model.

3.7. Effect of addition of hydrogen peroxide

The results from the degradation of the AO7 (20 mg l^{-1}) using different concentrations of H_2O_2 were summarized in Fig. 10. The removal efficiency increased with increasing H_2O_2 concentration, but the improvement was not obvious above 10 mM. This can be explained by the two opposing effects with increasing H_2O_2 concentration [3,4,18]:

(a) H_2O_2 reacts with the electrons which are emitted from valence band of the photocatalyst to generate hydroxyl radicals and hydroxide anions while inhibiting the e_{CB}^-/h_{VB}^+ recombination process:

$$H_2O_2 + e_{CB}^- \rightarrow OH^- + {}^\bullet OH \quad (13)$$

(b) H_2O_2 may also be split photolytically to produce hydroxyl radicals directly:

$$H_2O_2 + h\nu \rightarrow 2\,{}^\bullet OH \quad (14)$$

It should be taken into consideration that photocatalytic oxidation will be inhibited via reaction of excess H_2O_2 with $^\bullet OH$ radicals and h_{VB}^+:

$$H_2O_2 + {}^\bullet OH \rightarrow HO_2{}^\bullet + H_2O \quad (15)$$

$$HO_2{}^\bullet + {}^\bullet OH \rightarrow H_2O + O_2 \quad (16)$$

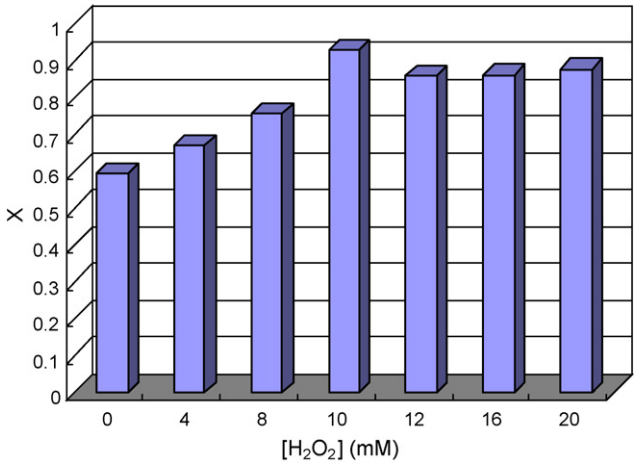

Fig. 10. Effect of H_2O_2 addition on photocatalytic degradation efficiency of AO7 at irradiation time of 15 min. $[AO7]_0 = 20\,\text{mg l}^{-1}$; $[ZnO] = 160\,\text{mg l}^{-1}$; pH neutral.

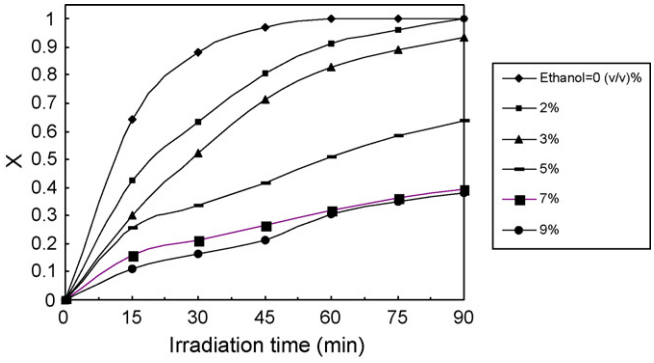

Fig. 11. Inhibition of photodegradation of AO7 ($20\,mg\,l^{-1}$) by ethanol. [ZnO] = $160\,mg\,l^{-1}$; pH neutral.

$$H_2O_2 + h_{VB}{}^+ \rightarrow H^+ + HO_2^\bullet \quad (17)$$

Therefore, high concentration of hydrogen peroxide inhibited the reaction rate of dye degradation by competing with AO7 for available hydroxyl radicals [13,19].

3.8. Effect of addition of ethanol

Alcohols such as ethanol are commonly used to quench hydroxyl radicals. The rate constant of reaction between hydroxyl radical and ethanol is $1.9 \times 10^9\,M^{-1}\,s^{-1}$ [3,4,16]. It was observed that small amounts of ethanol inhibited the photocatalytic degradation of AO7. Fig. 11 shows that addition of ethanol inhibits the photooxidative degradation of AO7. The retarding effect of ethanol in this system can be explained by $^\bullet$OH competitive reactions with AO7 and ethanol. This result showed that hydroxyl radicals play a major role in the UV/ZnO process [3,4].

3.9. Electrical energy efficiency

Science photodegradation of aqueous organic pollutant is an electric energy-intensive process, and electric energy can represent a major fraction of the operating costs, simple figures-of-merit based on electric energy consumption can be very useful and informative. Recently, the Photochemistry commission of the International Union of Pure and Applied Chemistry (IUPAC) proposed a figure-of-merit (or more appropriately, an efficiency index, as it compare electrical efficiency of different AOPs) for UV-based AOPs. It compares electrical efficiency of different UV-based AOPs and it is a measure of the electrical efficiency of an AOP system. It is defined (for low concentration of pollutants) as the electrical energy in kilowatt hours (kWh) required for bringing about the degradation of a contaminate by one order of magnitude in $1\,m^3$ of contaminated water [20]. Considering first-order degradation kinetics, the UV dose was calculated for each of the processes using Eq. (18). The EE/O values were obtained from the inverse of the slope of a plot of $\log(C_0/C)$ versus energy dose (kWh/m^3) using Eq. (19) [20,21]. The EE/O values for photocatalytic decolorization of C.I. Acid Orange 7 by UV/ZnO and UV/ZnO/H_2O_2 processes were 384 and $172\,kWh/m^3$, respectively.

$$\text{UV dose} = \frac{1000 \times \text{lamp power (kW)} \times \text{time (h)}}{\text{treated volume (l)}} \quad (18)$$

$$\text{EE/O} = \frac{\text{UV dose}}{\log(C_0/C)} \quad (19)$$

The EE/O values showed that a moderated efficiency was obtained in the UV/ZnO process. It is also clear that UV/ZnO/H_2O_2 process offered the best energy efficiency. In conclusion, the use of the H_2O_2 with optimized concentration (10 mM) in the UV/ZnO process can be extremely helpful in reducing the energetic cost of wastewater treatment [20–22].

4. Conclusion

The photocatalytic oxidation of AO7 has been studied using ZnO nanopowder as photocatalyst. Photocatalytic degradation of AO7 was negligible when ZnO nanopowder and UV light were used on their own. The results indicated that degree of degradation of AO7 was obviously affected by illumination time, pH and photocatalyst amount. We also learned that optimal amount of photocatalyst was $160\,mg\,l^{-1}$, with dye concentration of $20\,mg\,l^{-1}$. ZnO cannot be used at pH lower than 4. The photocatalytic decomposition of AO7 was most efficient in neutral solution. The complete removal of color, after selection of desired operational parameters, could be achieved in a relatively short time of about 60 min. From the inhibitive effect of ethanol, it was concluded that hydroxyl radicals were the main reactive species, but probably positive holes were also involved. With addition of oxidant into illuminated ZnO suspensions a synergistic effect was observed leading to an enhancement of the process except of the additional amount of hydrogen peroxide into ZnO suspension which causes a decrease to the rate of the reaction. The kinetic of photocatalytic removal of AO7 followed Langmuir–Hinshelwood model. The electrical energy consumption per order of magnitude for photocatalytic degradation of AO7 was lower in the UV/ZnO/H_2O_2 process than that in the UV/ZnO process.

Acknowledgement

The authors thank the University of Tabriz, Iran for financial and other supports.

References

[1] S. Chakrabarti, B.K. Dutta, Photocatalytic degradation of model textile dyes in wastewater using ZnO as semiconductor catalyst, J. Hazard. Mater. B 112 (2004) 269–278.
[2] V. Kandavelu, H. Katien, R. Thampi, Photocatalytic degradation of isothiazolin-3-ons in water and emulsion paints containing nanocrystalline TiO_2 and ZnO catalysts, Appl. Catal. B: Environ. 48 (2004) 101–111.
[3] A.A. Khodja, T. Sehili, J. Pilichowski, P. Boule, Photocatalytic degradation of 2 phenyl-phenol on TiO_2 and ZnO in aqueous suspension, J. Photochem. Photobiol. A: Chem. 141 (2001) 231–239.
[4] N. Daneshvar, D. Salari, A.R. Khataee, Photocatalytic degradation of azo dye acid red 14 in water on ZnO as an alternative catalyst to TiO_2, J. Photochem. Photobiol. A: Chem. 162 (2004) 317–322.

[5] B. Liu, T. Torimoto, H. Yoneyama, Photocatalytic reduction of CO_2 using surface-modified CdS photocatalysts in organic solvents, J. Photochem. Photobiol. A: Chem. 113 (1998) 93–97.
[6] I. Konstantinou, T. Sakellarides, V. Sakkas, T. Albanis, Photocatalytic degradation of selected S-triazine herbicides and organophosphorus insecticides over aqueous TiO_2 suspensions, Environ. Sci. Technol. 35 (2001) 398–405.
[7] Y.T. Kwon, K.Y. Song, W.I. Lee, G.J. Choi, Y.R. Do, Photocatalytic behavior of WO_3-loaded TiO_2 in an oxidation reaction, J. Catal. 191 (2000) 192–199.
[8] H. Lin, S. Liao, S. Hung, The dc thermal plasma synthesis of ZnO nanoparticles for visible-light photocatalyst, J. Photochem. Photobiol. A: Chem. 174 (2005) 82–87.
[9] S. Sakthivel, B. Neppolian, M.V. Shankar, B. Arabindoo, M. Palanichamy, V. Murugesan, Solar photocatalytic degradation of azo dye: comparison of photocatalytic efficiency of ZnO and TiO_2, Sol. Energy Mater. C 77 (2003) 65–82.
[10] W. Huihu, X. Changsheng, Z. Wei, C. Shuizhou, Y. Zhihong, G. Yanghai, Comparison of dye degradation efficiency using ZnO powders with various size scales, J. Hazard. Mater. B 112 (2004) 269–278.
[11] C. Lizama, J. Freer, J. Baeza, H. Mansilla, Optimal photodegradation of reactive blue 19 on TiO_2 and ZnO suspension, Catal. Today 76 (2002) 235–246.
[12] M.C. Yeber, J. Rodriguez, J. Freer, J. Baeza, N. Duran, H. Mansilla, Advanced oxidation of pulp mill bleaching wastewater, Chemosphere 39 (1999) 1679–1688.
[13] M.A. Behnajady, N. Modirshahla, R. Hamzavi, Kinetic study on photocatalytic degradation of C.I. Acid Yellow 23 by ZnO photocatalyst, J. Hazard. Mater. B 133 (2006) 226–232.
[14] X. Liu, X. Wang, J. Zhang, X. Hu, L. Lu, A study of nanocrystalline TiO_2 preparation with inorganotitantes and gelatin dispersant: thermal analysis of complex gel, Thermochim. Acta 342 (1999) 67–72.
[15] I.K. Konstantinou, T.A. Albanis, TiO_2-assisted photocatalytic degradation of azo dyes in aqueous solution: kinetic and mechanistic investigation, Appl. Catal. B: Environ. 49 (2004) 1–14.
[16] N. Daneshvar, D. Salari, A.R. Khataee, Photocatalytic degradation of azo dye acid red 14 in water: investigation of the effect of operational parameters, J. Photochem. Photobiol. A: Chem. 157 (2003) 111–116.
[17] J. Villasenor, H. Masilla, Effect of temperature on kraft black liquor degradation by ZnO-photoassisted catalysis, J. Photochem. Photobiol. A: Chem. 93 (1996) 205–209.
[18] A. Aleboyeh, H. Aleboyeh, Y. Moussa, Critical effect of hydrogen peroxide in photochemical oxidative decolorization of dyes: Acid Orange 8, Acid Blue 74 and Methyl Orange, Dyes Pigments 57 (2003) 67–75.
[19] N. Daneshvar, M.J. Hejazi, B. Rangarangy, A.R. Khataee, Photocatalytic degradation of an organophosphorus pesticide phosalone in aqueous suspension of titanium dioxide, J. Environ. Sci. Health B 39 (2) (2004) 285–296.
[20] N. Daneshvar, D. Salari, A. Niaei, M.H. Rasoulifard, A.R. Khataee, Immobilization of TiO_2 nanopowder on glass beads for the photocatalytic decolorization of an azo dye C.I. Direct Red 23, J. Environ. Sci. Health A 40 (2005) 1605–1617.
[21] N. Daneshvar, A. Aleboyeh, A.R. Khataee, The evaluation of electrical energy per order (E_{Eo}) for photooxidative decolorization of four textile dye solutions by the kinetic model, Chemosphere 59 (2005) 761–767.
[22] D. Salari, N. Daneshvar, F. Aghazadeh, A.R. Khataee, Application of artificial neural networks for modeling of the treatment of wastewater contaminated with methyl *tert*-butyl ether by UV/H_2O_2 process, J. Hazard. Mater. B 125 (2005) 205–210.